



ELSEVIER

1 April 2002

Optics Communications 204 (2002) 407–411

OPTICS
COMMUNICATIONS

www.elsevier.com/locate/optcom

Second-harmonic generation with broadened flattop bandwidth in aperiodic domain-inverted gratings

Zeng Xianglong*, Chen Xianfeng, Wu fei, Chen Yuping, Xia yuxing, Chen yingli

Department of Applied Physics, Institute of Optics and Photonics, Shanghai Jiaotong University, Shanghai 200240, P.R. China

Received 11 September 2001; received in revised form 3 January 2002; accepted 20 February 2002

Abstract

We report on a theoretical analysis for the broadened bandwidth of the fundamental waves in aperiodic gratings. The sequences and the length of the domains are optimized to realize the pre-designed wide bandwidth in the quasi-phase-matched (QPM) second-harmonic generation (SHG) by the simulated annealing (SA) method. About 3 nm prescribed flattop bandwidth as the full width at 95% maximum with 25% reduction of the nonlinear coefficient relative to that of a perfectly periodic QPM grating are obtained. Domains overgrown owing to the room-temperature electric poling technique show little influence on the broad bandwidth of the fundamental waves. © 2002 Published by Elsevier Science B.V.

PACS: 42.65.Ky

Keywords: Aperiodic domain-inverted gratings; Flattop bandwidth; Quasi-phase-matching

Quasi-phase-matching (QPM) in periodically poled LiNbO₃ (PPLN) and periodically domain-inverted AlGaAs is widely used for optical parametric processes such as generation of the short wavelength from infrared radiations and optical parametric oscillators because of its largest usable nonlinear optical coefficient and a wider range of phase-matchable wavelength compared with those of the conventional birefringence phase-matching techniques [1,2]. Besides, QPM can fulfill long

nonlinear interaction length between the interaction waves. As we know, the conversion efficiency increases quadratically with the interaction length while the bandwidth scales inversely with the length. But the narrow acceptance bandwidth for the fundamental wavelength and temperature, which exceeds the tolerances on laser diodes due to the fluctuation of laser wavelength or of temperature, or on errors in the fabrication process, critically limits the utility of the QPM technique [3].

The acceptance bandwidth may be increased by perturbing the QPM grating so that spectral components in wavevector domains can spread to the wings. Some schemes for broadening the phase-matching bandwidth in QPM second-harmonic

* Corresponding author. Tel.: +86-21-54743252; fax: +86-21-62932019.

E-mail address: zxlsjtu@263.net (Z. Xianglong).

(SH) generation devices have been proposed and investigated. One is the segmented grating, which makes use of located phase shifts inserted into a periodic grating [4,5], but this kind of structure needs fine adjustment of the period and the phase shifts. Others are the chirped grating [6] and the variable-spaced-phase-reversed grating [3], which both result in ripples more than 1 dB. However, broadening the flattop bandwidth with high conversion efficiency in aperiodic domain-inverted gratings has not yet been proposed.

In this paper, we propose, for the first time to the best of our knowledge, an approach to obtain the wide flattop bandwidth based on aperiodic domain-inverted gratings constructed with the opposite ferroelectric domains, whose lengths are less than the coherence length. Simulated annealing (SA) method [7–9] is applied to optimize the sequences of this ferroelectric-domain structure, which can provide plenty of reciprocal vectors to compensate for the wavevector mismatch between the interactive waves. Thus it may be expected that spectral components can continuously expand in a wide range of the wavevectors. These new structures offer greater design flexibility in the pre-designed broad bandwidths of SHG.

As is shown in Fig. 1, the sample is divided into layers with the equal thickness ΔL , and the total length of sample is $L = \Delta LN$. This structure can be fabricated by the room-temperature electric poling technique with pre-designed patterns or by GaAs/Ge/GaAs sublattice reversal epitaxy [1,2]. For convenience we take the bulk periodically poled LiNbO₃ for discussions. The length of each layer ΔL is less than the coherence length. The orientation of the domains, as the signs of nonlinear optical coefficient, and the sequence are determined

later by the specified calculated results. Different numbers of layers with the same orientation in successive sequence compose the positive or negative domains. In terms of the characteristic structure, the arrangement of the domains is irregular.

Let us consider SHG process for this aperiodic optical grating in the bulk LiNbO₃. Assume that a laser beam with the wavelength of λ is perpendicularly incident from the left of this grating and the second-harmonic field is generated. In the assumption of the slowly varying amplitude and the small-signal approximation, the amplitude of the second-harmonic field $E_2(\lambda)$ at the end of the sample of length L is given by [10]

$$E_2(L, \lambda) = \Gamma d_{\text{eff}} G[\Delta k(\lambda)], \quad (1)$$

where

$$\Gamma = i \frac{\omega}{n_2 c} E_1^2, \quad (2)$$

$$G[\Delta k(\lambda)] = \frac{1}{L} \int_0^L g(z) \exp[-i\Delta k(\lambda)z] dz.$$

Subscripts 1 and 2 refer to quantities associated with fundamental and harmonic waves respectively. Δk is the wavevector mismatch between the fundamental and second-harmonic waves $\Delta k(\lambda) = k_{2\omega} - 2k_\omega = \pi/l_c(\lambda)$, $l_c(\lambda)$ is the coherence length. $g(z) = d(z)/d_{\text{eff}}$ is the normalized structure function (where d_{eff} is the largest element of the nonlinear coefficient tensor, d_{33}). For the scheme described above, $g(z)$ only takes the binary values of ± 1 . From Eq. (2), in terms of Fourier transform, $G(\Delta k)$ is the spectrum function in the wavevector mismatch Δk domain of the space-dependent nonlinear coefficient function $g(z)$ in the space domain. The efficiency of the nonlinear

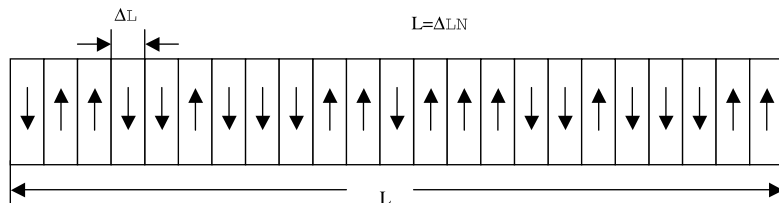


Fig. 1. Model of the QPM grating with aperiodic domains in part; the sign of the effective nonlinearity changes with the domain orientation and the sequence is determined by the specified calculated results. The total length is $L = \Delta LN$ and each layer equals ΔL .

interaction depends completely on the structure function and is proportional to $|G(\Delta k)|^2$. The broadened bandwidth requires that the Fourier transform $G(\Delta k)$ is a flattop function in wavevector mismatch domain. From Eq. (1), the amplitude of $G(\Delta k)$ represents the reduction in effective nonlinearity compared to that for the conventional QPM condition, which is also referred to the reduced effective nonlinear coefficient d_{reff} of the SHG [9].

According to our schematic drawing of a nonlinear structure above, d_{reff} can be expanded by

$$\begin{aligned}
 d_{\text{reff}}(\lambda) &= |G[\Delta k(\lambda)]| \\
 &= \frac{1}{N\Delta L} \left| \sum_{q=0}^{N-1} g(z_q) \int_{z_q}^{z_q+\Delta L} d\xi e^{-i(\Delta k(\lambda)\xi)} \right| \\
 &= \left| \text{sinc} \left(\frac{\Delta L\pi}{2l_c(\lambda)} \right) \right| \\
 &\times \left\{ \frac{1}{N} \sum_{q=0}^{N-1} g(z_q) \exp -i[\pi(q + 0.5)\Delta L/l_c(\lambda)] \right\}.
 \end{aligned} \tag{3}$$

The first factor is sinc function of $\Delta L\pi/2l_c(\lambda)$, where $l_c(\lambda)$ is the coherence length of the fundamental wavelength λ . For the perfect first order QPM, $\Delta L = l_c(\lambda)$, it equals $2/\pi$; when the length of each layer reduces by one-third, the value is increased to $3/\pi$, 50% greater than that of the perfect QPM condition. The second factor is determined by the interference effect of all domains, which is globally dependent on the sequences and the sign of every domain. The optimal results can be obtained by the SA method.

In our calculation, we adopt the length of each layer

$$\Delta L = \frac{l_c(1.55 \mu\text{m})}{3} \approx 3.40 \mu\text{m}$$

and $N = 3300$, the total length of the bulk lithium niobate is 11.22 mm and the refractive indices of the fundamental and second-harmonic waves are from the Sellmeier equation [11]. The bandwidth is pre-designed as 3 nm at 1.55 μm , i.e., the fundamental wavelength from 1.550 to 1.553 μm , which all can be all phase-matched to generate second-harmonic waves. The optimal consecutive order of domains is obtained by choice of the appropriate objective

function in the SA method. We scan this aperiodic grating with the use of the sampling wavelength from 1.54 to 1.56 μm with the step of 0.01 nm. The calculation results are shown in Fig. 2. With the optimized aperiodic structure, the flattop response of pre-designated bandwidth of wavelengths is achieved only at the expense of the reduced effective nonlinear coefficient 25% lower than that of the perfectly periodic QPM grating. For perfect QPM uniform grating, the ideal maximum value of the effective nonlinear coefficient should be 0.6366, whereas the bandwidth at 1.55 μm is only 0.31 nm as the full width at 95% maximum. With the same parameters, other preset bandwidths like 2 and 5 nm are also shown in Fig. 2. The effective nonlinear coefficient d_{reff} decreases as the bandwidth is broadened. This is because of the trade-off between the wide bandwidth and the conversion efficiency. From the above discussion, the wide bandwidth can be engineered in aperiodic domain-inverted gratings.

It is interesting to investigate the property of the performance of the wide bandwidth as the second-harmonic waves propagate along the aperiodic grating. The interference factor in Eq. (3) is consistent with the variation of the reduced effective coefficient along the propagation direction. The

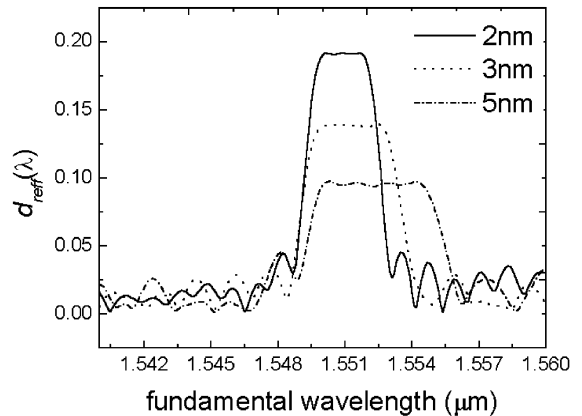


Fig. 2. Calculated broadened bandwidth with identical nonlinear optical coefficient for the aperiodic grating constructed by the specified calculated sequence of the orientation of each layer. $\Delta L = 3.40 \mu\text{m}$ and $N = 3300$. The prescribed bandwidth is 2, 3 and 5 nm respectively at fundamental wavelength around 1.55 μm .

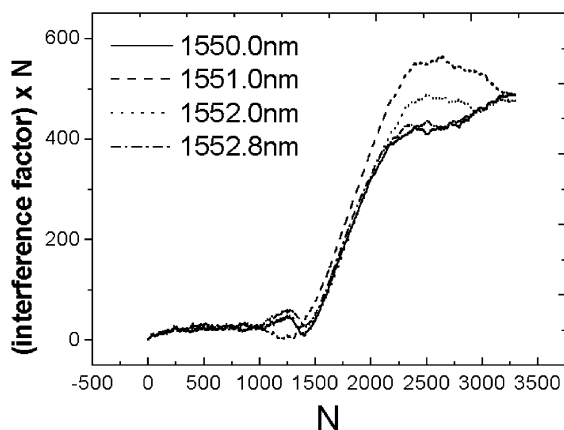


Fig. 3. The interference factor in Eq. (3) is consistent with the variation of the effective nonlinear coefficient along propagation direction versus the number of layers N . The wavelengths chosen for calculation are within the bandwidth shown in Fig. 2.

result is shown in Fig. 3. From the plot, each curve tends to the same end through different ways. This clearly manifests that the wavelengths in a wide bandwidth can all globally be phase-matched by the interference effect of all constructed domains, but undergo different interference processes.

We also investigate the effect of errors caused by the room-temperature electric poling process. As is well known, the inverted domains typically grow beyond the width of the metal electrode defined by pre-designed patterns [1]. Since the error of domain lengths is inevitable under the current room-temperature poling techniques, we take into account the resultant domain size after the poling process. We assume that the inverted domains extend its edge into adjacent layers of the opposite sign, and the noninverted domains correspondingly are shortened. The portion of the extended part to the length of each layer is denoted by μ . The influence of this extension by the fabrication process is depicted in Fig. 4. As μ increases, the effective nonlinear coefficient and the quality of flattop are reduced.

In summary, we have shown that the phase-matching bandwidth is broadened by using aperiodic domain-inverted gratings. From the viewpoint of Fourier transform, the physical mechanism for the broad bandwidth with high

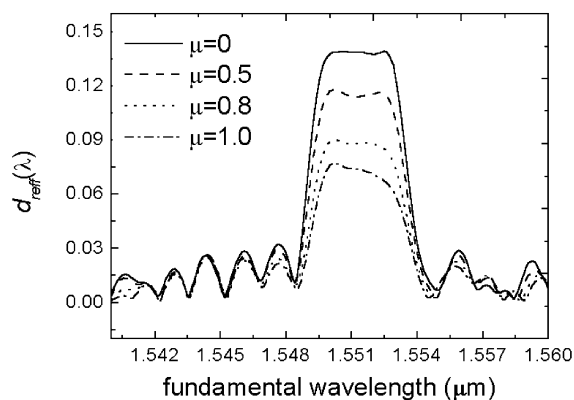


Fig. 4. Influence of domains overgrown outside of the metal edge in the constructed aperiodic grating in the case of the bandwidth of 3 nm at parameters of Fig. 2.

conversion efficiency has been analyzed theoretically. The aperiodic domain-inverted gratings can implement pre-designed flattop response with the optimum sequence of the orientation of each layer by the SA method. This method is not only useful in achieving the broad acceptance bandwidth of SHG, but also may be a promising approach for tunable devices.

Acknowledgements

This research was supported by the Fund of Technologic Development in Shanghai, People's Republic of China under the grant no. 99JC14011 and National Science Foundation of China. The authors wish to thank Prof. Li Qu for useful discussions.

References

- [1] L.E. Myers, R.C. Eckardt, M.M. Fejer, R.L. Byer, W.R. Bosenberg, J.W. Pierce, *J. Opt. Soc. Am. B* 12 (1995) 2102.
- [2] I. Shoji, T. Kondo, A. Kitamoto, M. Shiraneand, R. Ito, *J. Opt. Soc. Am. B* 14 (1997) 2268.
- [3] M.L. Bortz, M. Fujimura, M.M. Ferjer, *Electron. Lett.* 30 (1994) 34.
- [4] K. Mizuuchi, K. Yamamoto, M. Kato, H. Sato, *IEEE J. Quantum Electron.* 30 (1994) 1596.
- [5] K. Mizuuchi, K. Yamamoto, *Opt. Lett.* 23 (1998) 1880.

- [6] T. Suhara, H. Nishihara, *IEEE J. Quantum Electron.* 26 (1990) 1265.
- [7] Kirkpatrick, C. Dgelatt, M.P. Vecchi, *Science* 220 (1983) 671.
- [8] B.Y. Gu, B.Z. Dong, Y. Zhang, G.Z. Yang, *Appl. Phys. Lett.* 75 (1999) 2175.
- [9] B.Y. Gu, Y. Zhang, B.Z. Dong, *J. Appl. Phys.* 87 (2000) 7629.
- [10] M.M. Fejer, G.A. Magel, D.H. Jundt, R.L. Byer, *IEEE J. Quantum Electron.* 26 (1990) 1265.
- [11] D.H. Jundt, *Opt. Lett.* 22 (1997) 1553.